25th European Photovoltaic Solar Energy Conference and Exhibition /
5th World Conference on Photovoltaic Energy Conversion, 6-10 September 2010, Valencia, Spain

EMBEDMENT OF METAL NANOPARTICLES IN GaAs AND Si FOR PLASMONIC ABSORPTION ENHANCEMENT IN INTERMEDIATE BAND SOLAR CELLS

Manuel J. Mendes*, Estela Hernández, Ignacio Tobías, Antonio Martí and Antonio Luque
Instituto de Energía Solar, Universidad Politécnica de Madrid,
Avda. Complutense 30, 28040 Madrid, Spain
Corresponding author: manuel.mendes@ies-def.upm.es

ABSTRACT: The high near-field enhancement occurring in the vicinity of metallic nanoparticles (MNPs) sustaining surface plasmons can only be fully exploited in photovoltaic devices if the MNPs are placed inside their semiconducting material, in the photoactive region. In this work an experimental procedure is studied to embed MNPs in gallium arsenide (GaAs) and silicon (Si), which can be applied to other semiconductor host materials. The approach consists in spin-coating colloidal MNPs dispersed in solution onto the substrate surface. Then a capping layer of the same material as the substrate is deposited on top to embed the MNPs in the semiconductor. The extinction spectra of silver (Ag) and gold (Au) MNPs embedded in GaAs and Si is modeled with Mie theory for comparison with optical measurements.
This contribution constitutes the initial step towards the realization of quantum-dot intermediate band solar cells (QD-IBSC) with MNPs.
Keywords: Light Enhancement, Surface Plasmons, Nanoparticles

1 INTRODUCTION

In recent years there has been a growing interest in the optical properties of metal nanoparticles (MNPs) since they exhibit strong scattering resonance in the optical regime, at frequencies that can be tuned by engineering the particle size and shape. These excitations occur when the applied electromagnetic (EM) field frequency matches the frequency of the collective oscillations of the conduction electrons (plasmons). The free electrons in MNPs are strongly bound to the particle surface, thus the particle geometry significantly influences the frequency at which they oscillate. Therefore, in MNPs these excitations are usually known as localized surface plasmons (LSPs) [1].

At the LSP resonance the pronounced polarizability of the MNP effectively draws the energy supplied by an incident EM wave into the particle. This produces a scattered field whose evanescent electric-field component can have an intensity several orders of magnitude higher than that of the incident field [2]. This field component decays very rapidly with distance, so it is only significant in a close proximity of the MNP surface (within its near-field region).

Such enhanced local fields are drawing attention for use in optoelectronic devices such as LEDs [3] and photovoltaics (PV). In the case of PV, incorporating MNPs leads to a locally enhanced optical absorption and an overall increase in the power conversion efficiency. This has already been attempted mostly in thin-film [4], silicon [5,6] and organic [7] solar cells. However, due to fabrication constraints, most of these experimental approaches place the MNPs on top or in the bottom of the solar cells [8]. With such designs there is little interaction between the enhanced near-field around the MNP and the cell absorbing material; hence LSPs cannot markedly contribute to the photocurrent generation. The increase in absorption and current reported in these works is mainly a far-field effect, where the MNPs act similarly as conventional texturing to increase the optical path length and decrease reflection losses [9].

The LSP light enhancement can only be fully exploited if the MNPs are placed inside the cell photoactive material; because the region of highest scattered field occurs within a distance from the MNP of about the MNP size.

The authors are mainly interested in the implementation of MNPs inside the active region of intermediate band solar cells (IBSCs) [10]. The IBSC can generate photocurrent from sub-bandgap photons, without voltage degradation, due to the existence of an electronic band — the intermediate band (IB) — within the host semiconductor bandgap [11]. As such, the IBSC concept reaches a detailed balance efficiency limit of 63.2%, compared to 40.7% for conventional single-gap cells. The IB can be formed by the confined levels of a quantum dot (QD) array. Prototype QD-IBSCs were fabricated with ten InAs QD layers grown in GaAs [12]. However, the IB impact on the cell performance is still marginal, mainly due to the weak absorption coefficient associated to the QDs. One way of increasing this absorption is by making use of the high LSP near-field that can appear close to MNPs [13]. The inclusion of MNPs close to QDs can amplify their absorption by several orders of magnitude, as described in [10].

This paper presents the first step aimed at incorporating MNPs in QD-IBSCs. Here we focus on the experimental challenges related with the inclusion of an array of individual MNPs in the interior of typical semiconductor materials for solar cells: GaAs and Si. Nevertheless, the results given here can be applied to other types of solar cells with distinct semiconductor materials. We work with MNPs made of silver (Ag) or gold (Au), since these are two of the metals which exhibit the strongest plasmonic scattering at solar frequencies [14].

The scattering properties of MNPs are highly dependent on their size, shape, material and surrounding dielectric environment. Therefore, it is beneficial to use analytical techniques to model their optical response. In the experiments performed in this work spherical particles are used. Hence, their scattered fields can be computed with Mie theory [15]. After describing the fabrication details (section 2) a study is presented (section 3) of the extinction spectra of Ag and Au MNPs in GaAs and Si, in order to compare the computed results with optical measurements.

2 FABRICATION PROCESS

Our approach for embedding MNPs in a semiconductor consists in two main steps. First, an array of MNPs is patterned on a cleaned surface of the semiconductor wafer. Then, a capping layer of the same material as the wafer is deposited on top to cover the MNPs completely in the semiconducting medium.

The preferable MNP sizes for plasmonic light enhancement in solar cells are on the order of 10-100nm [10]. One way for patterning arrays of MNPs of such dimension is through e-beam lithography (EBL) followed by metal evaporation. EBL is currently the most accurate physical deposition method allowing nanometer precision in the control of the geometry and inter-particle spacing of the patterned objects. However, this technique is expensive, time consuming (it would take several days to pattern a small 2 inch wafer) and hardly scalable [16]. Therefore, most of the previously cited works that attach MNPs to the surface of solar cells use bottom-up techniques such as thin-film anneling [8]. This method is much more suited for large area devices, but there is a high non-uniformity in the size, shape and distribution of the patterned MNPs.

In this work a bottom-up wet coating process is developed to incorporate MNPs in photovoltaic devices. This consists in spin-coating colloidal MNPs dispersed in solution onto the substrate surface. It is possible to synthesize MNP dispersions of spherical particles with well-defined diameters; but it is still difficult to controllably engineer the shape of non-spherical objects such as spheroids. For application in IBSCs, oblate spheroidal MNPs are preferable since their LSP resonance is located deeper in the infrared than spheres [10]. However, MNPs with oblate geometries cannot currently be produced in colloidal solution. Therefore, for the initial studies reported in this work, we use spherical MNPs dispersed in pure water which were bought from *nanoComposix* company. The particles are coated with an atomic layer of tannic or citric acid that prevents their aggregation in water but does not significantly disturb their optical response.

In our process, each of the two main steps referred in the beginning of this section is divided into two sub-steps:

1) MNP Patterning:
   1.1) **Hydrophilization** – passivation of the wafer surface to make it wettable for the spin-coating
   1.2) **Spin-coating** - the colloidal MNPs solution is spin-coated onto the surface. The water is then evaporated by oven-drying, leaving only the MNPs array

2) Capping layer growth:
   2.1) **Wafer cleaning** - removal of organic contaminants, surface oxides and other impurities to prepare the surface for the next deposition step
   2.2) **Capping layer deposition** – a layer of the same material as the wafer is deposited on top, embedding the MNPs in the semiconductor

In the following sub-sections we shall describe in detail these four steps.

2.1 Surface hydrophilization and spin-coating

A distribution of isolated and uniformly-spaced MNPs can be achieved with spin-coating if the liquid in which the MNPs are dispersed wets the surface. In our case the liquid is water, which does not wet pure Si and GaAs surfaces (they're hydrophobic). So it is essential to chemically hydrophilize the surfaces of these materials before spin-coating.

Si wafers become perfectly hydrophilic after cleaning with the standard RCA procedures [17]. These acidic or basic solutions mixed with H_2O_2 leave on the Si surface an hydroxylated oxide with OH- groups [18]. Such surface is hydrophilic in nature and easily wetted by aqueous solutions. The hidroxylated oxide can later be removed after spin-coating by dipping the wafer in a dilute HF solution, as explained below in 2.2.

The RCA cleaning methods cannot be applied to GaAs since they etch its surface quite aggressively. After several chemical tests, the best way found by us to hydrophilize GaAs is to dip the wafer for 30s in $NH_4OH(25\%):H_2O_2(30\%):H_2O$ (1:1:5 volume ratio). This is the same solution as that of RCA1 method [17], but the immersion time here is much shorter and no heating should be applied to prevent the material from being excessively etched. The NH_4OH in this solution removes the native surface oxide of GaAs and leaves an hydroxylated surface [19]. It was observed that the GaAs surface only remains hydrophilic for a few minutes after this treatment. Therefore, the spin-coating of the MNP dispersion should be performed immediately after this hydrophilization step.

The employment of the previously described surface treatments allowed us to achieve uniform distributions of MNPs, deposited by spin-coating on Si and GaAs wafers. After spin-coating, each sample is dried in oven for 15min at 130ºC to evaporate all the water and leave only the nanoparticles. The density and uniformity of the deposited MNPs is examined by taking several atomic force microscopy (AFM) images at several spots along the wafers. Fig. 1 is an example of such AFM images.

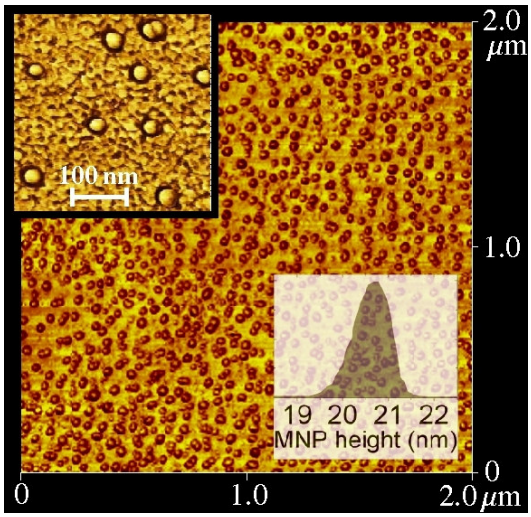

Figure 1: AFM phase image of 20nm Ag MNPs deposited by spin-coating on the surface of a GaAs wafer. The bottom inset is an histogram of the particles diameter (measured height).

Uniform MNP depositions have been obtained with Ag and Au MNPs on the surface of GaAs and Si. The density of the deposited MNP array can be controlled by varying the colloidal dispersion concentration and the rotation speed during spin-coating. As referred in section 1, the near-field region of pronounced light enhancement is located within a distance from the MNP surface of about its size. Therefore, in order to have complete in-plane near-field coverage with the least number of scatterers, the MNPs should be ideally spaced by a distance of about twice its diameter. The periodicity of the position of the deposited particles cannot be controlled by this technique. That would be important if inter-particle interaction effects were to be taken into account, which is not the case in the present study.

2.2 Surface cleaning after MNP deposition

After depositing the MNPs it is important to effectively clean the wafer surface without affecting the attached particles. This cleaning step should be able to remove any contaminants coming from the MNP solution and the superficial oxides in the Si and GaAs wafers.

To that end, a series of chemical tests have been conducted to study the robustness and adhesion strength of the deposited MNPs on Si and GaAs samples. After each test the sample surface was inspected by AFM to check if there was any size reduction or adsorption of the nanoparticles. It was observed that the relevant processes listed in Table I do not cause any considerable changes to the deposited particles.

Table I: Tested cleaning procedures that do not remove nor etch the deposited MNPs

	Process	Solvents	Time	Temp.
1	Degreasing with organic solvents	Acetone Isopropanol Methanol	3 min in each solvent	60 ºC
2	Bath Sonication	Acetone or DI water	1 hour	Room Temp.
3	Etching of GaAs oxides	NH_4OH (25% solution)	10 min	80 ºC
4	Light etching of SiO_2	HF (0.14% solution)	1 min	Room Temp.

Processes 1 and 2 should be able to remove any organic contaminants resulting from the spin-coating step. Whereas processes 3 and 4 remove, respectively, the surface oxides in GaAs [20] and Si [17]. The times used for the tests listed in Table I are above the minimum times required for each cleaning process. This way we can be sure that the MNPs do not suffer any change even if the process takes longer than the minimum necessary time.

2.3 Capping layer deposition – Thermal tests

The last fabrication step consists in the growth of a top layer, of Si or GaAs, to embed the nanoparticles in the semiconducting medium of the wafer. This can be performed by chemical vapour deposition, molecular beam epitaxy, or sputtering followed by thermal annealing. For GaAs growth these processes use temperatures in the range of 500-600ºC; whereas for Si growth the temperatures can go higher than that depending on the process used and the required degree of crystallinity.

In order to verify if the MNPs can withstand the growth of such capping layer, we have conducted a series of thermal tests to determine the maximum temperature that the nanoparticles can support without suffering any structural deformation. Four different MNP dispersions were deposited on distinct GaAs and Si substrates. The four dispersions we composed of Ag and Au particles with diameters of 20nm and 30nm.

A Solaris 75 Rapid Thermal Annealing (RTA) equipment was employed to heat all the samples at distinct temperatures between 200ºC and 1000ºC, during 20min. During the RTA the samples were in an inert atmosphere of forming gas (90% N_2 + 10%H_2) at atmospheric pressure.

After the RTA all the samples were inspected by AFM, at distinct spots along their surface, to see if there was any change in the deposited MNPs diameter (height).

It was observed that no size change occurs in the MNPs deposited on GaAs up to 500ºC. Above this temperature we cannot tell by AFM what occurs to the particles, since the As starts to desorb from the substrate leaving an excess of Ga on its surface [21]. This causes the appearance of holes on the surface and small droplets formed by the excess of Ga [22] which mask the MNPs and prevent us from accurately measuring their sizes.

Si substrates are more thermally stable since their surface remains smooth up to 1000ºC. From the AFM measurements of MNPs deposited on Si, we have concluded that the 20nm and 30nm Ag MNPs suffered no changes up to 700ºC, and the Au MNPs up to 800ºC. At higher temperatures the particles start vanishing, and at 1000ºC practically no particles are present. It is not possible to tell by AFM which physical mechanisms (sublimation, melting or diffusion into the substrate) are responsible for the disappearance of the MNPs; however, there are several other literature contributions that investigate this in further detail. Thermodynamic models assuming isolated spherical MNPs yield a linear relationship between the melting temperature and the reciprocal of the particle size [23,24]. It is predicted that isolated Ag and Au MNPs with diameters above 15nm should have a melting point very close (within 10% difference) to that of the bulk crystal (960ºC for Ag and 1063ºC for Au). However, most of these models do not consider the interaction with the substrate, which plays a crucial role on the thermal behavior of the deposited MNPs [25]. This surface interaction reduces the melting point of the nanoparticle, relative to that predicted for isolated particles, and can determine the physical mechanism responsible for the MNP size reduction with temperature.

The thermal limits of 700-800ºC observed here for MNP stability are well above the usual GaAs deposition temperatures (500-600ºC). Thus, the MNPs should not suffer any deformation during the GaAs capping layer growth. As for the Si capping layer growth, a deposition process should be chosen that keeps its temperature below the MNPs' thermal stability limit.

3 COMPUTATIONAL SCATTERING STUDIES

Scattering by individual spherical particles, such as the colloidal MNPs used in this work, can be computed analytically with Mie theory [26]. This is a separation of variables method that determines the exact solution of Maxwell's equations for the plane-wave scattering by a homogeneous sphere of arbitrary size. In the case of particles much smaller than the wavelength of incident light the simplified electrostratic approximation (EA) can be used [15]. This assumes that the whole object responds as an electric dipole to the applied EM field.

The materials considered for the nanoparticles are Ag and Au, embedded in a medium of Si or GaAs. The refractive index of these materials is interpolated from experimental data [27].

In practical experiments it is common to measure the LSP resonance of MNPs dispersed in water by taking the wavelength-resolved extinction (absorption+scattering) spectrum of the solution. The dashed lines of Fig. 2 show the spectra of five MNP dispersions with distinct particle diameter. At optical wavelengths water is practically transparent, so for each dispersion the observed extinction peak occurs at the average particles' LSP resonance. These extinction spectra can be modeled by computing the extinction cross section (Q_{ext}) with Mie theory, shown in the solid lines of Fig. 2. The refractive index of water was taken to be 1.33.

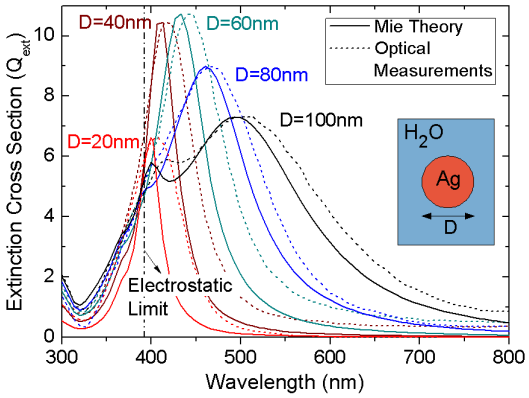

Figure 2: Extinction cross section (solid lines) of individual Ag spheres in water with distinct diameters (D), computed with Mie theory. These are compared with optical extinction measurements (dashed lines) performed by *nanoComposix* on their MNP dispersions. The units of the measured extinction are arbitrary; thus the dashed curves are normalized to the corresponding Q_{ext} peak intensity, for better visualization. The vertical dash-dot line corresponds to the LSP wavelength calculated with the EA approach, for particles much smaller than the wavelength

The optical response of small MNPs is predominantly dipolar in nature, but as the particle size is increased retarded potentials cause the field inside the particle to become less uniform. This leads to the excitation of higher-order modes (quadrupolar, octopolar, etc.) with different scattering characteristics and higher resonance frequencies [28]. For instance, in Fig. 2 a clear quadrupolar peak is present in the spectrum of 100nm MNPs (black line) at a wavelength close to 400nm.

In a GaAs or Si medium the Q_{ext} peaks are red-shifted relative to those in water, since the refractive index of these materials (≈3.5 in the infrared) is higher than water. This is shown in Fig. 3a) for GaAs, where it can be seen that the LSP resonance appears close to the GaAs bandgap (1.43eV) for diameters below 40nm. The Q_{ext} spectra of MNPs with D>50nm presents additional higher-order peaks besides the dipolar LSP resonance. As the particle size increases the magnitude of these peaks increases relative to that of the dipole mode. In the case of 100nm MNPs in GaAs (black line) it is the quadrupolar peak that shows the maximum Q_{ext}.

In Fig. 3b) it can be seen that the dipolar LSP resonance occurs at very similar frequencies for Ag and Au MNPs in GaAs and Si. Differences are observed in the maximum Q_{ext} only for big particles when higher-order modes become dominant.

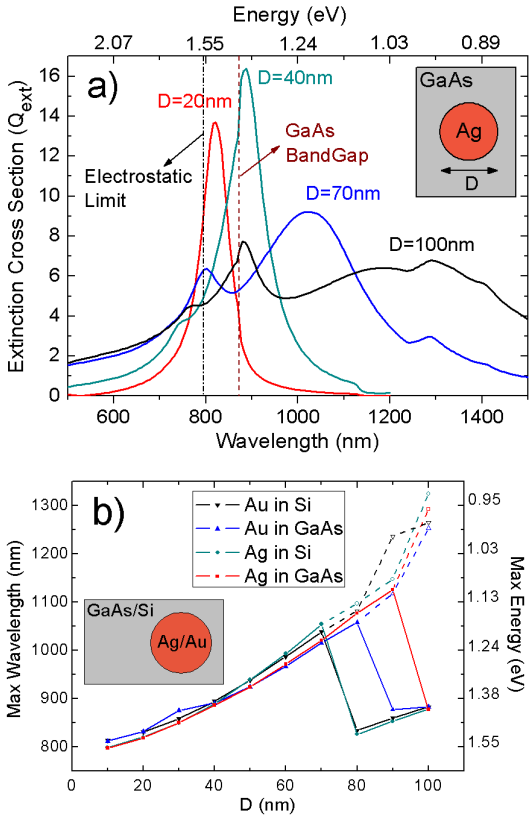

Figure 3: **a)** Extinction cross section (Q_{ext}) spectra of Ag spheres in GaAs, computed with Mie theory. The vertical black dash-dot line corresponds to the LSP wavelength calculated with EA. **b)** Maximum Q_{ext} wavelengths, as a function of MNP diameter, for Ag and Au MNPs embedded in GaAs or Si. For big sizes the Q_{ext} maxima no longer occur at the dipolar resonances (shown along the dashed-lines) but switch to higher-order modes, such as in the case of D=100nm in a).

4 CONCLUSIONS AND FUTURE WORK

In this work a scalable process is presented to introduce an array of uniformly-spaced spherical MNPs, with well-defined sizes, in the interior of GaAs and Si. This constitutes an initial step towards the realization of

quantum-dot intermediate band solar cells (QD-IBSC) with MNPs placed in the QD layers, as proposed in [10].

The first part of the method consists in the hydrophilization of the wafer surface so that the MNP colloidal dispersion can effectively be deposited by spin-coating. After spin-coating the surface can be cleaned by several processes that do not remove the MNPs and make it ready for the last step – the capping layer deposition that embeds the MNPs in the semiconductor material. It was observed that Ag MNPs with sizes of 20 and 30nm can withstand temperatures up to 700ºC without suffering any deformation; while Au MNPs with the same sizes can go up to 800ºC. These thermal limits should not constitute an impediment to the growth of the GaAs or Si capping layer on top of the deposited MNP array.

The studies performed so far use uncoated MNPs. However, MNPs coated with a dielectric shell (silica, for instance) should have a better thermal and electrical performance. Silica-coated MNPs were seen to withstand higher temperatures without structural changes [29]. This is because the shell creates a barrier between the MNP and the substrate, reducing the surface effects on the particle thermal deformation. Besides, the dielectric shell acts as a passivation coating on the MNP, preventing electron-hole recombination at the metal surface. A silica shell a few nanometers thick should prevent current degradation due to recombination and still allow a sufficiently high scattered field intensity [10].

The authors are now engaged in the last step of this process: the capping layer deposition on top of MNP-covered wafers. The samples are then going to be analyzed optically using transmission, photo-luminescence and photo-reflectance measurements. In a future contribution a comparison shall be presented between the optically measured LSP resonances of MNPs in Si and GaAs and the computed Mie theory results given in section 3.

ACKNOWLEDGEMENTS

We would like to thank Dr. José M. Ripalda for assistance with the AFM measurements.

This work has been supported by the IBPOWER Grant No. 211640 of European Commission, by the GENESIS FV grant CSD2006-0004 of the Spanish program CONSOLIDER, and by the NUMANCIA grant S-0505/ENE/0310 of “Comunidad de Madrid”. M. J. Mendes acknowledges the Portuguese Government fellowship SFRH/BD/21669/2005 of the “Fundação para a Ciência e Tecnologia – Ministério da Ciência, Tecnologia e Ensino”, and the Beca Homologada CH/007/2010 of “Universidad Politécnica de Madrid”.

REFERENCES

[1] Stefan Maier, *Plasmonics: Fundamentals and Applications*. (Springer, Berlin, 2007).
[2] A. Luque, A. Marti, M. J. Mendes et al., Journal of Applied Physics 104 (2008) 8.
[3] S. Pillai, K. R. Catchpole, T. Trupke et al., Applied Physics Letters 88 (2006) 3.
[4] Y. A. Akimov, W. S. Koh, and K. Ostrikov, Optics Express 17 (2009) 10195.
[5] F. J. Beck, S. Mokkapati, A. Polman et al., Applied Physics Letters 96 3.
[6] F. J. Beck, A. Polman, and K. R. Catchpole, Journal of Applied Physics 105 (2009) 7.
[7] S. S. Kim, S. I. Na, J. Jo et al., Applied Physics Letters 93 (2008) 3.
[8] F. J. Beck, S. Mokkapati, and K. R. Catchpole, Progress in Photovoltaics: Research and Applications (2010) n/a.
[9] J. Y. Lee and P. Peumans, Optics Express 18 (2010) 10078.
[10] M. J. Mendes, A. Luque, I. Tobias et al., Applied Physics Letters 95 (2009) 3.
[11] A. Luque and A. Marti, Physical Review Letters 78 (1997) 5014.
[12] A. Luque, A. Marti, C. Stanley et al., Journal of Applied Physics 96 (2004) 903.
[13] A. Urbanczyk, G. J. Hamhuis, and R. Notzel, Applied Physics Letters 97 (2010) 043105.
[14] L. Novotny and B. Hecht, *Principles of Nano-Optics*. (Cambridge University Press, Cambridge, UK, 2006).
[15] C. F. Bohren and D. R. Huffman, *Absorption and scattering of light by small particles*. (Wiley-VCH, Weinheim, 2004).
[16] S. Pillai and M. A. Green, Solar Energy Materials and Solar Cells 94 (2010) 1481.
[17] L. Muhlhoff and T. Bolze, Fresenius Zeitschrift Fur Analytische Chemie 333 (1989) 527.
[18] Karen A. Reinhardt and Werner Kern, (William Andrew Publishing, 2008).
[19] Zaijin Li and et al., Journal of Semiconductors 31 (2010) 036002.
[20] C. Bryce and D. Berk, Industrial & Engineering Chemistry Research 35 (1996) 4464.
[21] M. Yamada and Y. Ide, Surface Science 339 (1995) L914.
[22] C. Y. Lou and G. A. Somorjai, Journal of Chemical Physics 55 (1971) 4554.
[23] T. Castro, R. Reifenberger, E. Choi et al., Physical Review B 42 (1990) 8548.
[24] H. M. Lu, P. Y. Li, Z. H. Cao et al., Journal of Physical Chemistry C 113 (2009) 7598.
[25] C. L. Chen, J. G. Lee, K. Arakawa et al., Applied Physics Letters 96 (2010) 3.
[26] Max Born and Emil Wolf, *Principles of Optics: Electromagnetic Theory of Propagation, Interference and Diffraction of Light (7th Edition)*. (Cambridge University Press, 1999).
[27] Edward Palik, *Handbook of Optical Constants of Solids (5 Volume Set)*. (Academic Press, San Diego, CA, 1997).
[28] T. L. Temple, G. D. K. Mahanama, H. S. Reehal et al., Solar Energy Materials and Solar Cells 93 (2009) 1978.
[29] Y. S. Chen, W. Frey, S. Kim et al., Optics Express 18 (2010) 8867.